



## Poly(vinylidene chloride)-Based Carbon as an Electrode Material for High Power Capacitors with an Aqueous Electrolyte

M. Endo,<sup>a,z</sup> Y. J. Kim,<sup>a</sup> T. Takeda,<sup>a</sup> T. Maeda,<sup>a</sup> T. Hayashi,<sup>a</sup> K. Koshiba,<sup>a</sup> H. Hara,<sup>a</sup> and M. S. Dresselhaus<sup>b</sup>

<sup>a</sup>Faculty of Engineering, Shinshu University, Nagano 380-8553, Japan

<sup>b</sup>Department of Physics and Department of Electrical Engineering and Computer Science, Massachusetts Institute of Technology, Cambridge, Massachusetts 02139, USA

The specific capacitance (F/g) of a poly(vinylidene chloride) (PVDC)-based electric double-layer capacitor (EDLC) carbon electrode prepared by heat-treatment at only 700°C shows a capacitance as high as 64 F/g at 1 mA output current density, although it shows a specific surface area of only 700 m<sup>2</sup>/g, smaller than those of other conventional activated carbon fibers and activated carbons. To elucidate the relationship between the specific capacitance and the pore structure for PVDC-based carbons, from an EDLC practical applications viewpoint, structural characterization was performed using various techniques. PVDC-based carbon had sufficient porosity during the carbonization process without any additional activation process for use as an EDLC electrode. It has been shown that the strongest peak in the pore size distribution is at a diameter around 9 Å. The most probable electrolyte ion sizes, solvated as the hydrated SO<sub>4</sub><sup>2-</sup> ions in aqueous solution, have been obtained by computer simulation as 9 Å. This range of electrolyte ion sizes is highly convenient for entering the pores of the present PVDC-based carbons to establish the electric double layer at the pore wall. Furthermore the evolution of Cl<sub>2</sub> and HCl during the carbonization of PVDC creates rich open pores with nanometer dimensions connecting to the free surface of the particles in the samples. It is concluded that the higher specific capacitance of PVDC-based carbons, compared to conventional activated carbons in aqueous electronic double-layer capacitors, is due to their optimal pore size distribution. The present precursor has been shown to be a promising material for high power EDLC applications.

© 2001 The Electrochemical Society. [DOI: 10.1149/1.1401084] All rights reserved.

Manuscript submitted November 21, 2000; revised manuscript received June 22, 2001. Available electronically September 4, 2001.

Electric double-layer capacitors (EDLCs) have been used as a small scale energy storage device in electronic stationary applications, such as memory back-up devices and solar batteries with a semipermanent charge-discharge life cycle.<sup>1-5</sup> The EDLC device consists of polarized anode and cathode electrodes made of activated carbon, having a large specific surface area, with an aqueous or organic electrolyte. The capacitance (F) stored in this system is described by Eq. 1

$$C = \int \frac{\epsilon_0}{4\pi\delta} dS \quad [1]$$

where  $\epsilon_0$  is the dielectric constant of the electrolyte,  $\delta$  is the thickness of an electric double layer and,  $S$  is the surface area of the interface, respectively. Materials with granular or fibrous forms of carbons, having high specific surface area (SSA, m<sup>2</sup>/g), have been used as polarizable electrodes because of their larger working surface area as well as their relatively high electric conductivity. Extensive investigations to increase the specific capacitance (per weight and per volume) have been tried in various ways,<sup>6</sup> in order to expand EDLC applications in the field of hybrid electric vehicles (HEV), load leveling of electric power, and as promising high power energy storage devices.

In the present paper, a new type of carbon electrode for an aqueous EDLC, that is able to store a high power density, has been demonstrated. Generally, activated carbon materials have been prepared by an activation process, which includes an oxidizing process using steam or CO<sub>2</sub> and KOH, after the stabilization or carbonization processing steps. We have used a saran resin of poly(vinylidene chloride) (PVDC, —CH<sub>2</sub>CCl<sub>2</sub>—) as the starting material, because it can be obtained with a porous structure without any additional activation process, by using a heat-treatment that only yields carbonization. This material has been applied for use in aqueous EDLCs with 1 M H<sub>2</sub>SO<sub>4</sub> solution. Conventional activated carbons, which have a SSA as large as 1500-2000 m<sup>2</sup>/g or more, have been used to form an EDLC because of the relatively high conductivity of carbon as well as the high SSA of activated carbons (ACs). But the conventional

commercialized AC activated carbon fiber (ACF) electrodes have a lower capacitance than that of carbonized PVDC electrodes, even though they have much higher SSA. In the present paper, the specific EDLC properties of PVDC-based carbons are presented and the nanopore structure is discussed. This result could contribute to emphasizing the performance of specific EDLCs with aqueous as well as organic electrolytes from the viewpoint of the pore design for practical EDLCs.

### Experimental

The samples were prepared from PVDC (CH<sub>2</sub>CCl<sub>2</sub>), using various heat-treatment temperatures (HTT) in the range 300-1000°C with an inert atmosphere of N<sub>2</sub> and using an electric furnace for the heat-treatment. These samples were used for structural analysis and EDLC measurements. The process of electrode preparation for the EDLCs was as follows: the PVDC heat-treated at 400°C and 40 wt % of pristine PVDC as a binder were mixed and solubilized in tetrahydrofuran (THF) and then the solvent was removed by drying at room temperature in air. The samples were subsequently pressed into the shape of a disk, 12.4 mm in radius and 0.7 mm in thickness, using a steel-mold-type pressure apparatus operating at 3000 kgf/cm<sup>2</sup>. In order to get the fully carbonized EDLC electrode, the pellets were again heat-treated also at 700°C for 1 h.

The following measurements were performed to characterize the structure of the original PVDC-based carbon: thermogravimetric analysis (TGA), differential scanning calorimetry (DSC), X-ray diffraction (XRD), transmission electron microscopy (TEM, JEM-2010, JEOL), SSA measurements, the specific capacitance (F/g, F/cm<sup>3</sup>), and equivalent series resistance measurements. In particular, the specific capacitance (F/g) of various kinds of conventional activated carbons was also measured as a function of the specific surface area in order to compare with the present PVDC-based carbons.

Figure 1a illustrates the experimental cell used for the aqueous electrochemical double layer capacitor, in which identical electrodes for the cathode and anode were adopted for the cell configuration. PVDC-based carbon electrodes were set up in a glass beaker as an anode and cathode, with 30 wt % sulfuric acid aqueous solution. Before the capacitance measurement, each electrode was treated under primary vacuum conditions at room temperature for more than 14 h to remove the residual air remaining in the electrode and in the

<sup>z</sup> E-mail: endo@endomribu.shinshu-u.ac.jp

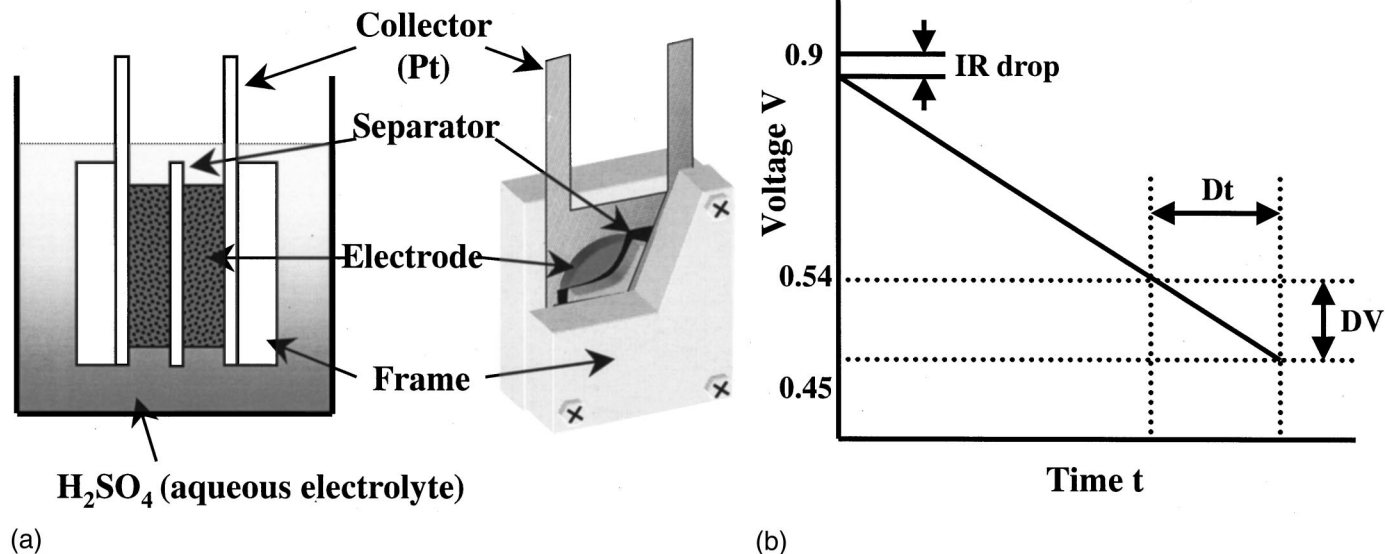


**Figure 1.** Cell construction and the method of capacitance measurement; (a, left) configuration of measurement cell, (b right) schematic discharge curve of the electric double-layer capacitor for capacitance measurement.

impregnated cell containing the electrolyte. Platinum plates were attached mechanically to the electrode samples for the output terminal. Glass paper (Oribest) was used as a separator. By using a similar system, various kinds of conventional AC and ACFs have been measured for their specific capacitance as a function of SSA at 0.9 V charge voltage and 1 mA discharge current. Also, other various types of ACs have been evaluated regarding their specific capacitance. To prepare a typical sample, 40 mg of AC/ACF material was mounted on a Pt plate and then pressed to make enough electric contact to measure the capacitance. The capacitance measurements were carried out using a constant voltage charge-constant current discharge method.

### Results and Discussion

Figure 2 shows the results of thermogravimetric analysis (TGA) of PVDC under flowing nitrogen gas. The weight variation of the sample occurred at the two distinct temperatures of 236.2 and 476°C (indicated by arrows), and the carbon yield obtained at 1000°C HTT was about 14.86%. The reasons for the two separate and distinct regions are expected to be related to the different binding energies of the C-Cl bond (328 kJ/mol), which breaks first, and to the subsequent breakage of the C-H bond (413 kJ/mol).<sup>7</sup>

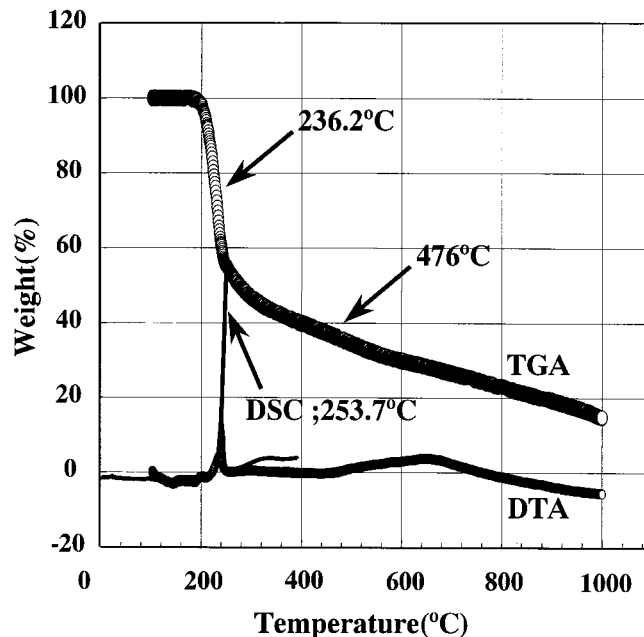
In the low temperature region of HTT (200-300°C), the weight of the carbon residue decreases markedly (70% of the total weight loss), due to the release of chlorine (Cl<sub>2</sub>) and hydrogen chloride (HCl) molecules. It is thought that the extensive gas release in the sample induces the formation of an open microporous structure in the resultant carbonaceous materials. Another weight loss, observed at relatively high HTT at 476°C, might originate from the loss of hydrogen, which presumably creates the nanopores, which are observed in the pore characterization studies described later.

Figure 3 shows the XRD profiles of PVDC-based carbons as a function of HTT from 700 to 1000°C. All samples show a broad XRD line at  $d_{002}$ , indicating a typical nongraphitizable carbon. Two broad lines are seen in the patterns, near  $2\theta \cong 24$  and  $44^\circ$ , corresponding to the 002 and 10 peaks, respectively. These results show that the carbons have no three-dimensional graphitic structure, and the computed apparent crystallite thickness  $L_c$  and  $d_{002}$  (d-spacing) are about 12 and 3.95 Å, respectively. These show that PVDC-based carbons are recognized as a material of very low crystallinity.

Table I shows a summary of the pore analysis results obtained from a Brunauer-Emmett-Teller (BET) study of the samples. The table demonstrates a tendency that the SSA increases with increas-

ing HTT, reaching a maximum surface area (771.92 m<sup>2</sup>/g) at HTT 800°C, and then decreases again. Lower SSA for samples heat-treated above 800°C might originate from a more completely developed carbon structure. That is, the pore formation caused by the release of the chlorine and hydrogen gas gradually decreases with increasing heat-treatment temperature. Thus, the SSA also decreases, but the average pore diameters show no variation with HTT and are more or less insensitive to heat-treatment after the gas is released.

As illustrated in Fig. 4a, the adsorption isotherms show type I behavior except for the sample heat-treated at 300°C. All the other samples studied here show isotherm behavior that is well identified as a microporous-based characteristic, the meso- and macroporosity being negligible. On the other hand, the sample heat-treated at



**Figure 2.** The TGA, DTA, and DSC profiles of weight percent vs. temperature obtained for PVDC.

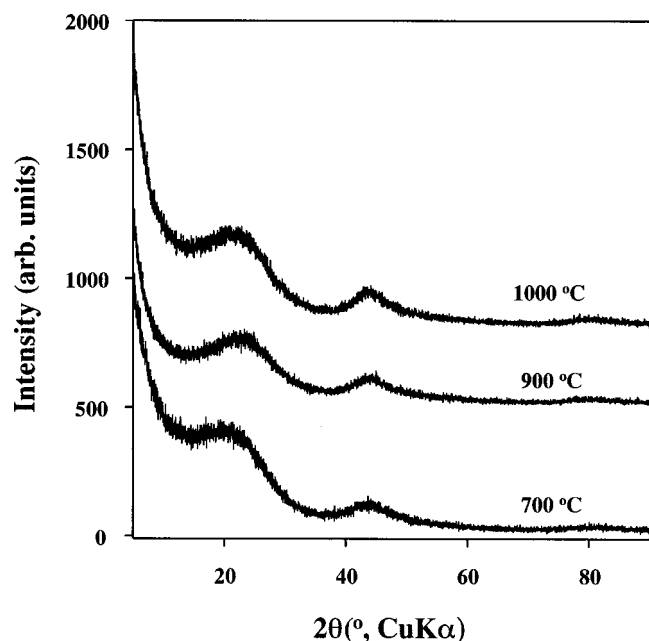
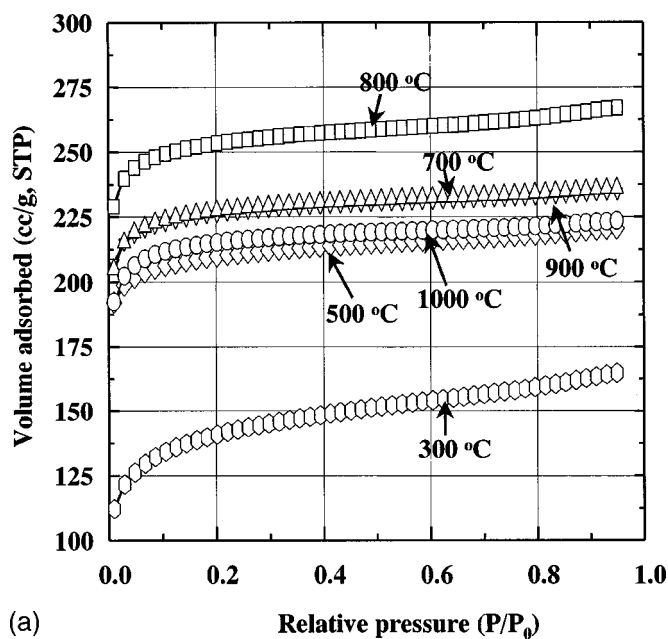


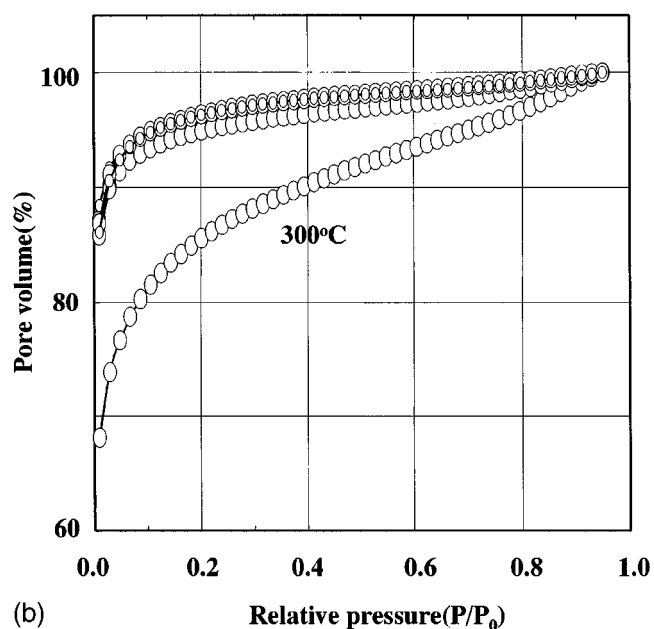
Figure 3. XRD profiles of PVDC-based carbons heat-treated at 700, 900, and 1000°C.

300°C shows a somewhat different profile. The point, called the B point indicating the relative pressure where the adsorbed species reaches a critical magnitude, shows a difference in the adsorption rate where it starts to adsorb. Figure 4b shows the isotherms converted to a percentage (%) of pore volume against the maximum partial pressure. This plot clarifies the difference between the behavior of 300°C HTT samples and the others, where the former evidently shows the isotherm for the 300°C to be closer to type II. These differences might originate from a porous structure of the HTT 300°C sample that is not developed enough. The isotherms for PVDC-based carbons show a remarkably large gas uptake at relative pressures in the range 0.01-0.3, possibly due to the presence of a large volume of micropores. It is thought that this adsorption occurs by a cooperative pore filling mechanism by molecules in a monolayer coating of the pore walls.<sup>5</sup> The sample heat-treated at 300°C shows a lower slope for the adsorption isotherm in this pressure range as compared with those of the other samples.

Figure 5 presents the pore-size distribution (PSD) of the samples, which was determined by application of the Cranston-Inkley (CI) equation.<sup>9</sup> These results indicate that the sample heat-treated at 700°C has its highest intensity peak around 9 Å, and another broad peak is observed around 16 Å in pore diameter, but with a lower intensity, less than that of any of the other samples. In other words, the HTT 700°C sample has a microporous structure dominated by pores of around 10 Å, as compared with the other samples. Measurements of the PSD were also tried by means of image analysis of



(a)



(b)

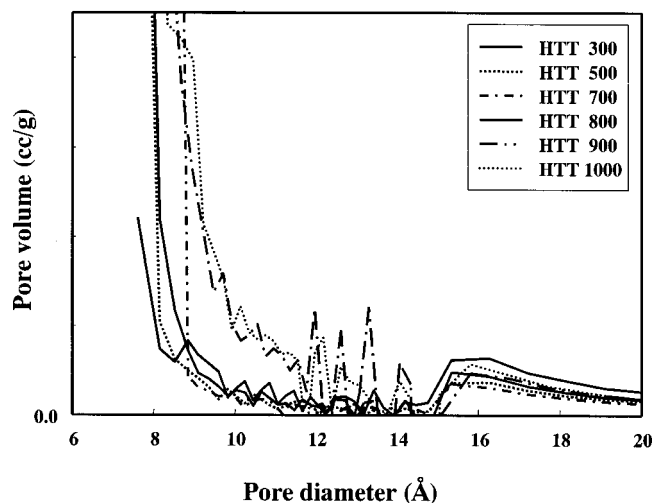
Figure 4. Adsorption isotherms of PVDC-based carbons heat-treated at various temperatures: (a, top) amount of adsorption vs. relative pressure ( $P/P_0$ ), (b, bottom) pore volume converted into percent vs. relative pressure ( $P/P_0$ ).

Table I. The results of BET analysis for SSA, total pore volume, average pore diameter of PVDC-based carbon materials heat-treated to various temperatures.

BET characteristics	HTT <sup>a</sup>					
	300°C	500°C	700°C	800°C	900°C	1000°C
SSA <sup>b</sup> (cm <sup>2</sup> /g)	442.63	640.66	617.01	771.92	692.64	659.90
Total pore volume (cm <sup>3</sup> /g)	0.25	0.34	0.33	0.41	0.37	0.35
Average pore diameter (Å)	15.62	14.62	14.44	14.69	14.48	14.48

<sup>a</sup> Heat-treated temperature.

<sup>b</sup> Specific surface area.



**Figure 5.** Pore size distribution (PSD) of PVDC-based carbons obtained by the CI method.

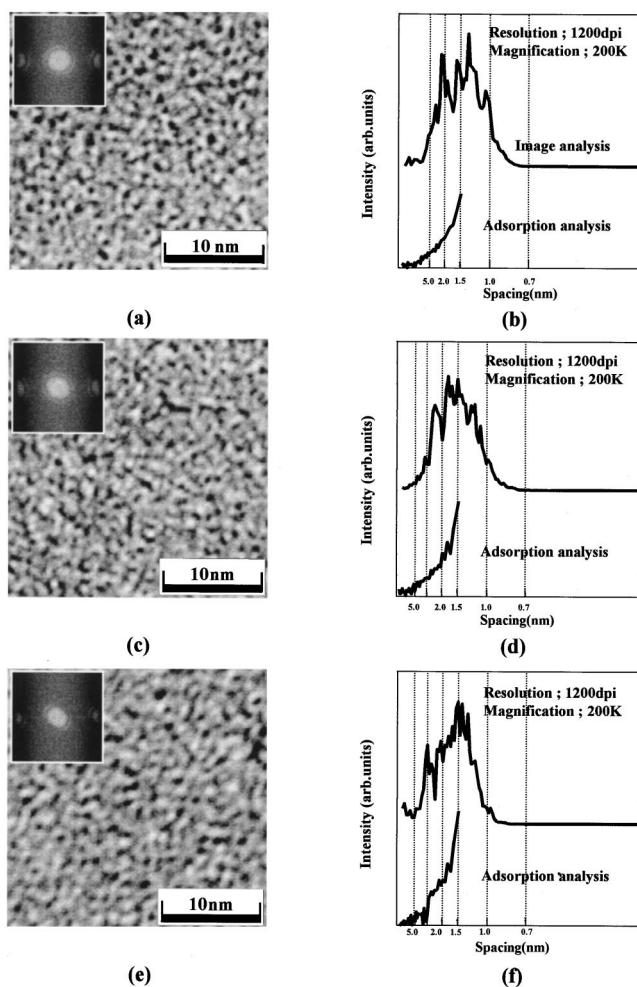
TEM micrographs. The TEM image obtained at 200,000 times magnification ( $\Delta f = 512$  nm) was converted to a  $512 \times 512$  pixel, 8 bits grayscale image in order to perform the 2D-FFT. The 2D power spectrum thus obtained showed no sign of anisotropy of the specimen. Thus, we can integrate the strength of the 2D power spectrum around the concentric circles that are centered at the center of the image to get the 1D integrated spectrum. The 1D integrated spectrum has the pore diameter preferentially aligned along the  $x$  axis, and the intensity of each value is evaluated along the  $y$  axis, to obtain the PSD.

Figure 6 shows high-resolution TEM images and the corresponding pore size distributions of PVDC-base carbon samples in comparison to the PSD obtained from the adsorption isotherms. The results show the existence of large numbers of nanopores with diameters less than 1 nm. Figures 6b, d, and f show the PSDs obtained by image analysis of the TEM pictures, using the corresponding FFT patterns for each picture.<sup>10,11</sup> The  $x$  axis denotes the spatial wavelength, and the  $y$  axis denotes the intensity of the power spectrum. In this figure, it is shown that the pore size is shifted toward larger sizes with increasing HTT, and that the dominant pore sizes are less than 1.5 nm for all three cases.

The pore-size distributions obtained by image analysis are quite consistent with those of the  $N_2$  adsorption isotherms. As mentioned above, it is certain that PVDC-based carbon has a porous structure with a pore-size distribution that is rather smaller than that of activated carbons which use only a carbonization step, and which could be more suitable for EDLC applications.

The EDLC test was discharged at 10 mA of constant current, and charged at 0.9 V of constant voltage for 5 min. Figure 1b shows a schematic discharge curve for the experimental cell with an aqueous electrolyte. The capacitance of the cell was calculated from the time period,  $\Delta t$ , which corresponds to a voltage change,  $\Delta V$ , taken from 0.54 to 0.45 V (from 60 to 50% of the initial voltage) under constant current discharge conditions. When the discharge starts using constant current, an initial voltage drop (IR drop) originating from the internal resistance (called the equivalent series resistance, ESR) of the cell was evaluated. To avoid any effect of the internal resistance on the capacitance, the capacitance measurement was carried out during the voltage drop ranging from 0.54 to 0.45 V by using the following equation

$$C = (I \times \Delta t) / \Delta V \quad [2]$$



**Figure 6.** TEM photographs and PSD curves obtained by image analysis; (a) and (b) PVDC-700°C; (c) and (d) PVDC-800°C; (e) and (f) PVDC-1000°C.

where  $C$  is the capacitance (F),  $I$  is the constant output current (A),  $\Delta t$  is the discharge time (s), and  $\Delta V$  is potential change (V), respectively.

Figure 7 shows the specific capacitance per unit weight (F/g) as a function of the output current density for various PVDC-based carbon bulk electrodes. The specific capacitance for each sample is observed to decrease with increasing current density. It is worth while to note, in particular, that the PVDC-based carbon 1000°C sample shows an extremely high efficiency for the variation of the current density. The figure shows that the PVDC-based carbon 700°C showed the largest capacitance of 64 F/g at a low current density of 1 mA, although the PVDC-800°C sample had a larger specific surface area than that of PVDC 700°C. The other samples have capacitance values in the order of PVDC-800 > 900 > 500 > 1000. The higher the heat-treatment temperature, the better is the maintenance of the specific capacitance with increasing current density. For example, the sample heat-treated at 1000°C shows the best maintenance of current density at 1 A/cm<sup>2</sup>, with a value of 34%. This current density stability seems to be related to the equivalent series resistance (ESR) and to the increase of the pore volume, with a mean pore size of 15 Å in the electrode.

Figure 8 shows the results of ESR after the measurement of the capacitance. It is shown that the ESR decreases with increasing heat-treatment temperature.

These PVDC-based carbon electrode samples have a much smaller specific surface area than those of typical ACF/AC (~2000 m<sup>2</sup>/g) (Fig. 9), but nevertheless show a two times higher capaci-

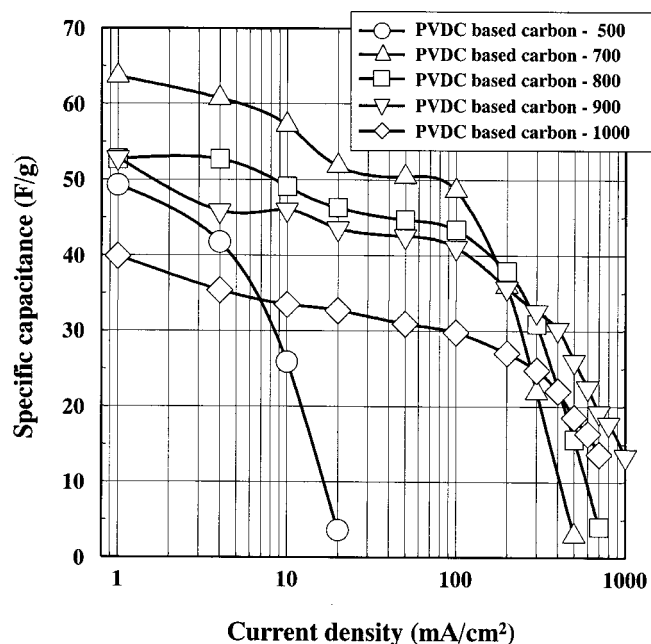


Figure 7. Specific capacitance (F/g) as a function of output current density for various PVDC-based carbon samples.

tance. This result can be related to the relative size difference between the pore and the electrolyte ion. As observed in Fig. 5 and 6, the capacitance for this sample is dominated by ultramicropores of less than 10 Å size.

The  $\text{H}_2\text{SO}_4$  electrolyte separates into a  $\text{H}^+$  ion and a  $\text{SO}_4^{2-}$  ion in aqueous solution. The  $\text{H}^+$  ion, with a very small size can easily participate in a repeated insertion and departure process. For the case of the  $\text{SO}_4^{2-}$  ion, it was considered as a possible structure of a hydrated sulfate. There could be various kinds of solvated sulfate species, such as  $6(\text{SO}_4^{2-}(\text{H}_2\text{O})_6)$  and  $12[\text{SO}_4^{2-}(\text{H}_2\text{O})_{12}]$ . According to a simulation by a semiexperimental calculation, these species have ion sizes of around 10 Å, indicating that these sulfate ions can fit into a pore having a typical size of around 10 Å. Such a relative range in size between the pore and the inserted ion into the pore seems to be best for getting a high capacitance.

A new consideration of pore structure is required for the problem about ion size, that is, we start from the idea of a different pore

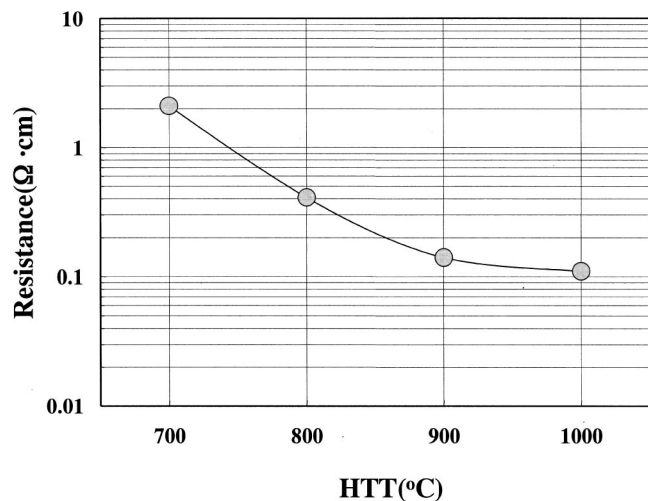


Figure 8. ESR vs. HTT for PVDC-based carbon.

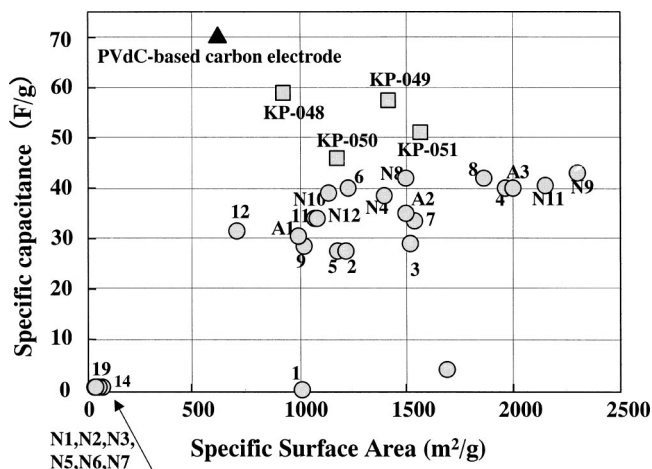


Figure 9. Specific capacitance as a function of specific surface area using various ACF/AC and PVDC-based carbons.

model based on the fractal theory to obtain the relation between ions for double-layer capacitance and pore size. The theory in the conventional parallel plate condenser has been applied, and the structure of the pore which exists in the interior of activated carbon was also assumed ideally to resemble slits and tubes, etc. However, real pores are quite different from the ideal structures according to the TEM observation. Therefore, we tried to clarify the real morphology of the pores by TEM. From the results of the TEM observation, it was confirmed that the real pores have a complicated contact surface that can be expressed with a fractal.<sup>10-12</sup> In the conventional model for the capacitance in the pore, the ideal structures is very applicable, but the real structure of ACF/AC is very complicated according to the result of TEM observation. Therefore, we proposed a new model on the basis of the real structure revealed by TEM.<sup>10,12</sup> This model provides information on the behavior of solvated ions in the pore. When the solvated ion size is large, the molecule cannot enter the pore. When the solvated ion size is small, it can go to the deep section of the continuous pore. The pores exist in the activated carbon material in a structure which can be expressed with a fractal, because the starting material of the activated carbon material is composed of randomly oriented microscopic carbon layers. These partial imperfections in the carbon layers are fractal and appear in the TEM image. Especially, PVDC-based carbon material has a shallow pit and/or pore. According to the experimental results, the size of 9-10 Å was found to give the optimum specific capacitance as electrodes. Pores of this size are also found by TEM image analysis. Consequently, we propose the size of 9-10 Å as a proper pore size or the diameter of the curved carbon surface as an electrode for EDLC based on the results of TEM image and computer simulation. In other words there are many pores and/or imperfections 9-10 Å in size and these play a role like an active site for ion storage and adsorption of solvated ion molecules.

Figure 9 shows a summary of results for capacitance measurements as a function of SSA for various AC/ACFs and carbonized PVDCs that were measured under 1 mA charge and discharge current. At this point, it is concluded that the PVDC-based electrodes show a higher capacitance than those of commercial AC/ACFs materials, which is reflected in the suitable pore size for the  $\text{H}_2\text{SO}_4$  aqueous electrolyte, by investigating the relation between the capacitance and the PSD of the host material.<sup>13</sup>

## Conclusions

In the present paper, a carbonized PVDC electrode, with an optimum porous structure, dominated by ultramicropores less than 10 Å in size without using any activation process, was used as the electrode of an EDLC in a sulfuric acid aqueous solution. This

PVDC-based carbon electrode performance showed a high capacitance of 64 F/g, even though the material has a smaller specific surface area than those of conventional ACF/AC materials. This result can be explained by the relation between the pore size distribution of the sample and the electrolyte ion size. PVDC-based carbons have a favorable pore size distribution for this application, based on various characterization methods. Besides the lower equivalent series resistance, a higher efficiency electrode can be obtained with this material. The present PVDC-based carbons exhibit an especially suitable pore size and pore size distribution with a higher bulk density that induces a high specific capacitance, which also can provide various technical merits in device applications. It is further possible to develop large-scale capacitor production using the present PVDC-based polarizable carbons.

#### Acknowledgments

Part of the work by M. Endo was supported by a grant-in-aid for "Research for the Future Program," Nano-carbon, from the Japan Society for the Promotion of Science.

#### References

1. M. Endo, in Extended Abstracts of the 24th Biennial Conference on Carbon, p. 522, Charleston, SC, USA, American Carbon Society (1999).
2. B. E. Conway, *J. Electrochem. Soc.*, **138**, 1539 (1991).
3. S. Trasatti and P. Kurzweil, *Platinum Met. Rev.*, **38**, 46 (1994).
4. M. Endo, Y. Okada, and H. Nakamura, *Synth. Met.*, **34**, 739 (1989).
5. S. Sarangapani, B. V. Tilak, and C.-P. Chen, *J. Electrochem. Soc.*, **143**, 3791 (1996).
6. S. T. Mayer, R. W. Pekala, and J. L. Kaschmitter, *J. Electrochem. Soc.*, **140**, 446 (1993).
7. T. W. G. Solomons, *Organic Chemistry*, 5th ed., Chap. 7, John Wiley & Sons, Inc., New York (1992).
8. S. J. Gregg and K. S. W. Sing, *Adsorption, Surface Area and Porosity*, 2nd ed., Chap. 4, Academic Press, London (1982).
9. R. W. Cranston and F. A. Inkley, *Adv. Catal.*, **9**, 143 (1957).
10. K. Oshida, K. Kogiso, K. Matsubayashi, K. Takeuchi, S. Kobayashi, M. Endo, M. S. Dresselhaus, and G. Dresselhaus, *J. Mater. Res.*, **10**, 2507 (1995).
11. M. Endo, T. Furuta, F. Minoura, C. Kim, K. Oshida, G. Dresselhaus, and M. S. Dresselhaus, *Supramol. Sci.*, **5**, 261 (1998).
12. M. Endo, K. Takeuchi, Y. Sasuda, K. Matsubayashi, K. Oshida, and M. S. Dresselhaus, *Electron. Commun. Jpn., Part 2: Electron.*, **77**, 98 (1994).
13. M. Endo, K. Oshida, K. Kogiso, K. Matsubayashi, K. Takeuchi, S. Kobayashi, and M. S. Dresselhaus, *Mater. Res. Soc. Symp. Proc.*, **371**, 511 (1995).